

## Preliminary Communication

Moustafa T. Gabr\*

# Antioxidant, $\alpha$ -glucosidase inhibitory and *in vitro* antitumor activities of coumarin-benzothiazole hybrids

<https://doi.org/10.1515/hc-2018-0101>

Received June 18, 2018; accepted August 10, 2018; previously published online September 10, 2018

**Abstract:** Coumarin-benzothiazole hybrids are antitumor agents based on their antioxidant and  $\alpha$ -glucosidase inhibitory activities. Compounds **5a–c** were selected by National Cancer Institute (NCI), USA, to be screened for antitumor activity at a single dose (10  $\mu$ M) against a panel of 60 cancer cell lines. The most active compound **5c** was further screened at a five-dose level by NCI. Compound **5c** displays half maximal growth inhibition ( $GI_{50}$ ) values of 0.24 and 0.33  $\mu$ M against central nervous system (CNS) cancer (SNB-75) and ovarian cancer (OVCAR-4) cell lines, respectively. Compounds **5a–c** were also screened for their antioxidant and  $\alpha$ -glucosidase inhibitory activities.

**Keywords:** antitumor activity; benzothiazoles; coumarins; hybridization; pharmacophore.

Glycosidases are a class of carbohydrate-hydrolase enzymes that catalyze hydrolysis of glycosidic bonds in oligosaccharides [1, 2]. The development of  $\alpha$ -glycosidase inhibitors with potential therapeutic applications has received considerable attention recently [3, 4]. The emergence of drug resistance to cancer chemotherapeutic agents has directed significant research efforts toward development of new agents for cancer treatment utilizing molecular hybridization (MH) strategy of different pharmacophores with the aim of obtaining superior anticancer activity compared to the parent molecules [5–7]. Limited examples of lead compounds from natural sources display promising antitumor activity based on their potent glycosidase inhibition activity [8].

The imbalance between overproduction of reactive oxygen species (ROS) and cellular detoxification

machinery in favor of ROS production, known as oxidative stress, leads to cellular damage and malfunction [9, 10]. Oxidative stress is directly associated with cancer progression, and there is a pressing need for development of potent antioxidant agents that can protect cellular organelles from ROS [11]. In this context, coumarin derivatives demonstrate intriguing antioxidant activity owing to scavenging of the initial radicals and propagating peroxy radicals [12, 13]. Moreover, coumarin-based compounds show promising antitumor activity [14] and are potent inhibitors of  $\alpha$ -glycosidase [15, 16]. Benzothiazole is a versatile synthetic scaffold with a wide spectrum of biological effects including potential antioxidant [17] and antitumor [18] activities. In addition, benzothiazole-containing agents show  $\alpha$ -glycosidase inhibitory activity [19, 20].

Bromophenols (BPs), isolated from marine algae, demonstrate promising  $\alpha$ -glycosidase inhibitory activity which has been attributed to the presence of bromo and hydroxy substituents [21, 22]. Therefore, BPs are promising lead compounds for the design of potential  $\alpha$ -glycosidase inhibitors. Bis(2,3-dibromo-4,5-dihydroxybenzyl) ether (BDDE, Figure 1) is a potent  $\alpha$ -glycosidase inhibitor with a half maximal inhibitory concentration ( $IC_{50}$ ) value of 0.098  $\mu$ M [21] and a potential antitumor agent [23]. Investigation of the binding interactions between BDDE and  $\alpha$ -glycosidase has identified a charged-hydrophobic-polar (C-H-P) binding pocket in  $\alpha$ -glycosidase that fits BDDE [24]. The hydroxy groups of BDDE are involved in multiple hydrogen bonds with residues in the polar areas of the binding pocket, while the rest of the molecule is stabilized by hydrophobic interactions with nearby residues. The binding mode of BDDE to  $\alpha$ -glycosidase is consistent with the structure-activity relationship established for hydroxycoumarin derivative (Figure 1) as potent  $\alpha$ -glycosidase inhibitor with  $IC_{50}$  values in the nanomolar range [25]. It is proposed that hydrogen bonding and extensive hydrophobic interactions in a cooperative fashion are involved in the  $\alpha$ -glycosidase inhibitory activity of the hydroxycoumarin derivatives. The basis of the cooperative hydrogen bonding and hydrophobic interactions has been derived from X-ray

\*Corresponding author: Moustafa T. Gabr, Department of Medicinal Chemistry, Faculty of Pharmacy, Mansoura University, Mansoura 35516, Egypt; and Department of Chemistry, University of Iowa, Iowa City, IA 52242, USA, e-mail: gabr2003@gmail.com

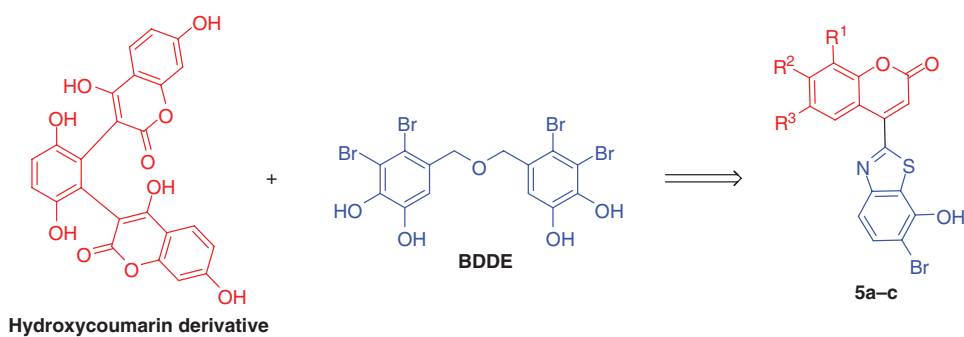


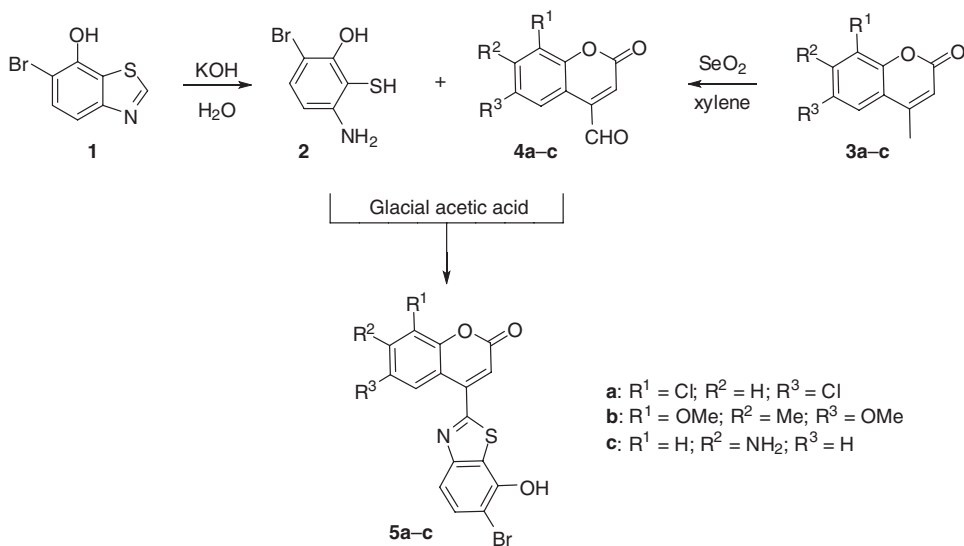
Figure 1  $\alpha$ -Glycosidase inhibitors reported in the literature and coumarin-benzothiazole hybrid compounds 5a-c.

crystallographic analysis of maltose in a complex with *Thermotoga maritima*  $\alpha$ -glucosidase AglA [26]. In the crystal structure, one of the glucose rings of maltose is bound by multiple hydrogen bonds to charged residues in the binding pocket, while the rest of the molecule is hydrophobically stacked to stabilize the interactions.

In this investigation, the design strategy of the coumarin-benzothiazole hybrids as  $\alpha$ -glycosidase inhibitors (Figure 1) interrogates structural features of both the marine natural BDDE and coumarins. It was anticipated that the benzothiazole core with bromo and hydroxy substituents would be implicated in hydrophobic and hydrogen-bonding interactions with  $\alpha$ -glycosidase similar to BPs. The coumarin moiety in the new hybrid compounds was speculated to be involved in additional hydrophobic and hydrogen bonding interactions in the hydrophobic and polar areas of the binding pocket. The synthesized coumarin-benzothiazole hybrids (Figure 1) were evaluated for their antitumor and antioxidant activities.

The target compounds 5a-c of this study were synthesized according to the general approach outlined in Scheme 1. As can be seen, the starting aminothiophenol 2 was synthesized by hydrolysis of the benzothiazole 1 with aqueous potassium hydroxide. Treatment of methyl substituted coumarin derivatives 3a-c with selenium dioxide in xylene proceeded smoothly to furnish formyl derivatives 4a-c in serviceable yields. Subsequent condensation of 2 and 4a-c in glacial acetic acid yielded coumarin-benzothiazole hybrids 5a-c (Scheme 1).

Compounds 5a-c were evaluated by the National Cancer Institute (NCI) *in vitro* for their antitumor activity [27]. A single dose (10  $\mu$ M) of the tested compounds was used in the full NCI-60 cell lines panel assay. Compounds 5a,b exhibited weak antitumor activity against all tested cell lines except for moderate activity of 5a against central nervous system (CNS) and breast cancer cell lines. Compound 5c displayed lethal effects (>100% inhibition) against non-small-cell lung cancer (HOP-62), CNS cancer



Scheme 1 Synthesis of compounds 5a-c.

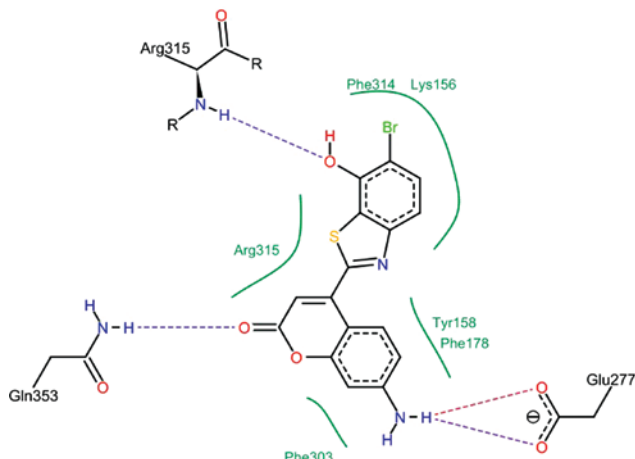


**Figure 2** Interaction of compound **5c** with the binding site of the target enzyme. Dashed lines represent hydrogen bonds. Hydrophobic interactions are shown by green solid lines.

(SNB-75) and ovarian cancer (SK-OV-3) cell lines. Subsequently, compound **5c** after passing this primary antitumor assay was carried over to the NCI five-dose screening. It can be suggested that the presence of a polar ionizable group on the coumarin moiety of these coumarin-benzothiazole hybrids is essential for antitumor activity. Potent antitumor activity of **5c** was evident against CNS cancer (SNB-75) and ovarian cancer (OVCAR-4) cell lines with half maximal growth inhibition values of 0.24 and 0.33  $\mu\text{M}$ , respectively.

Compounds **5a–c** were also evaluated for their *in vitro*  $\alpha$ -glucosidase inhibitory activity [28]. The results showed that compound **5c** exhibits promising inhibitory activity with an  $\text{IC}_{50}$  value of  $6.32 \pm 0.51 \mu\text{M}$  in comparison to miglitol as a reference compound ( $\text{IC}_{50} = 0.39 \pm 0.02 \mu\text{M}$ ). Compounds **5a,b** display moderate  $\alpha$ -glucosidase inhibitory activity with  $\text{IC}_{50}$  values of  $38.9 \pm 1.43$  and  $21.47 \pm 0.91 \mu\text{M}$ , respectively.

Antioxidant activities of compounds **5a–c** were determined using diphenylpicrylhydrazyl (DPPH) radical scavenging method [29]. In this test, compound **5c** displayed moderate antioxidant activity with an  $\text{IC}_{50}$  value of  $35.17 \pm 1.34 \mu\text{M}$  which is comparable to the activity of the standard reference ascorbic acid ( $\text{IC}_{50} = 22.8 \pm 0.71 \mu\text{M}$ ). Compounds **5a,b** displayed similar antioxidant capacity with  $\text{IC}_{50}$  values of  $44.5 \pm 2.66$  and  $41.36 \pm 2.12 \mu\text{M}$ , respectively. The correlation between antitumor activity of **5c** to its  $\alpha$ -glucosidase inhibitory and antioxidant activities in comparison to **5a,b** suggests that these activities represent the basis of its antitumor profile.

*Saccharomyces cerevisiae* isomaltase crystal structure (PDB ID: 3AJ7) shows high sequence similarity (72.4%) with  $\alpha$ -glucosidase and was utilized in this

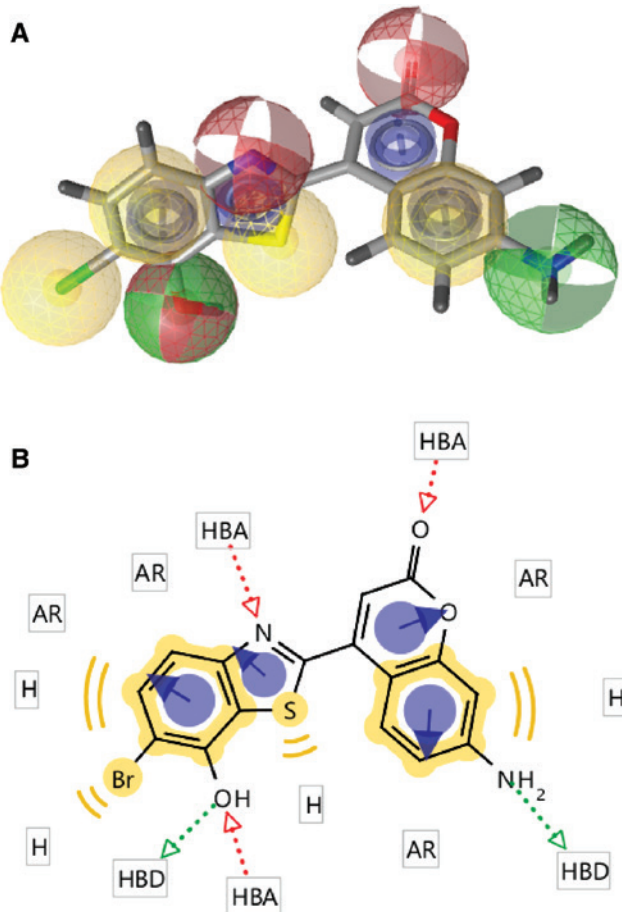


**Figure 3** The 3D and 2D pharmacophore maps of compound **5c**. (A) The 3D pharmacophore map; the pharmacophore color coding is red for hydrogen acceptor, yellow for hydrophobic regions and green for hydrogen donors. (B) The 2D pharmacophore map; HBA is hydrogen bond acceptor, H is hydrophobic center, HBD is hydrogen bond donor and AR is aryl.

investigation for molecular docking studies. Compound **5c** displays significantly preferential binding to the target enzyme with an estimated binding energy of  $-21.59 \text{ kcal mol}^{-1}$ , which is in good agreement with the result of the *in vitro*  $\alpha$ -glucosidase inhibition assay. The detailed analysis of the binding interaction is displayed in the two-dimensional (2D) binding mode of **5c** in Figure 2. As can be seen, the coumarin moiety of **5c** is stretched into a hydrophobic pocket of the target enzyme revealing hydrophobic interactions with Phe303, Phe178 and Tyr158. The carbonyl group of the coumarin scaffold interacts by hydrogen bonding with Gln353. It is noteworthy to mention that hydrogen bonding of the amino group in **5c** with Glu277 further stabilizes embedding of the coumarin moiety in the hydrophobic pocket, compared to **5a,b** that lack this interaction. The benzothiazole moiety of

**5c** is involved in  $\pi$ - $\pi$  interactions with Phe314 and Lys156, as well as hydrogen bonding with Arg315 (Figure 2).

Three-dimensional (3D) and 2D pharmacophoric maps for the structural features of compound **5c** (the most active member of this study) were created by Ligand-Scout software and are presented in Figure 3A and B, respectively. The investigated pharmacophoric features include hydrogen bond donors and acceptors as directed vectors, positive and negative ionizable regions as well as lipophilic areas that are represented by spheres. These pharmacophoric maps of **5c** may help design more potent antitumor coumarin-benzothiazole hybrids.

In conclusion, coumarin-benzothiazole hybrids **5a–c** were introduced in this investigation as a novel scaffold of potential antitumor agents. The substitution pattern of the coumarin moiety in the new hybrid molecules greatly affects their biological activity. Compound **5c** is the most active member of this study according to NCI's single- and five-dose assays. Intriguing antioxidant and  $\alpha$ -glucosidase inhibitory activities of **5c** are in good agreement with the antitumor screening results. The preliminary results reported in this study may help design new coumarin-benzothiazole hybrids as antitumor agents based on the nature and number of polar substituents on the coumarin nucleus.

## Experimental

$^1\text{H}$  NMR (400 MHz) and  $^{13}\text{C}$  NMR (100 MHz) spectra were recorded in  $\text{CDCl}_3$  on a Bruker spectrometer. Melting points were recorded using a capillary melting point apparatus and are uncorrected. HRMS were obtained in positive ion mode using ESI on a double-focusing magnetic sector mass spectrometer.

The antitumor screening of compounds **5a–c** [27], the  $\alpha$ -glucosidase inhibition assay [28], the antioxidant assay [29] and molecular modeling [30] were conducted as previously described.

**3-Amino-6-bromo-2-mercaptophenol** A mixture of compound **1** (1.15 g, 5 mmol) and KOH (2.80 g, 50 mmol) in water (10 mL) was heated at reflux overnight, then cooled and neutralized with 1 N HCl. The resultant precipitate was subjected to column chromatography eluting with 5% methanol in dichloromethane to give **2** as a dark yellow solid; yield 59%; mp 115–117°C;  $^1\text{H}$  NMR:  $\delta$  4.16 (bs, 1H), 4.95 (s, 2H), 6.59 (d, 1H,  $J$ =7.5 Hz), 7.12 (d, 1H,  $J$ =7.5 Hz), 8.85 (s, 1H);  $^{13}\text{C}$  NMR:  $\delta$  114.3, 117.4, 118.2, 125.8, 140.1, 159.1. HRMS. Calcd for  $\text{C}_6\text{H}_7\text{BrNO}_2$ ,  $[\text{M}+\text{H}]^+$ :  $m/z$  219.9431. Found:  $m/z$  219.9439.

**6,8-Dichloro-2-oxo-2H-chromene-4-carbaldehyde (4a)** A mixture of compound **3a** (2.29 g, 10 mmol) and selenium dioxide (1.23 g, 11.1 mmol) in xylene (100 mL) was heated at reflux overnight. The solvent was removed under reduced pressure and the crude product was subjected to silica gel column chromatography eluting with 2% methanol in dichloromethane to give **4a** as a light yellow solid; yield 72%; mp 130–132°C;  $^1\text{H}$  NMR:  $\delta$  6.81 (s, 1H), 7.18 (s, 1H), 7.75 (s, 1H),

9.94 (s, 1H);  $^{13}\text{C}$  NMR:  $\delta$  120.6, 122.4, 125.1, 128.9, 132.3, 133.5, 139.4, 152.3, 158.6, 192.6.

### 6,8-Dimethoxy-7-methyl-2-oxo-2H-chromene-4-carbaldehyde (4b)

Using the procedure for the preparation of **4a**, the reaction of **3b** (2.34 g, 10 mmol) and selenium dioxide (1.23 g, 11.1 mmol) gave **4b** as a yellow solid after purification by silica gel column chromatography using 2% methanol in dichloromethane as eluent; yield 87%; mp 137–139°C;  $^1\text{H}$  NMR:  $\delta$  2.19 (s, 3H), 3.51 (s, 3H), 3.58 (s, 3H), 6.65 (s, 1H), 6.90 (s, 1H), 9.98 (s, 1H);  $^{13}\text{C}$  NMR:  $\delta$  10.2, 59.5, 60.1, 118.1, 122.1, 123.5, 127.8, 130.2, 134.8, 141.9, 143.8, 155.4, 190.4.

### 7-Amino-2-oxo-2H-chromene-4-carbaldehyde (4c)

Using the procedure given for the preparation of **4a**, the reaction of **3c** (1.75 g, 10 mmol) and selenium dioxide (1.23 g, 11.1 mmol) gave **4c** as a yellow solid after purification by silica gel column chromatography using 5% methanol in dichloromethane as eluent; yield 51%, mp 155–157°C;  $^1\text{H}$  NMR:  $\delta$  6.62 (s, 2H), 6.81 (s, 1H), 6.95 (s, 1H), 7.38 (d, 1H,  $J$ =8.0 Hz), 7.70 (d, 1H,  $J$ =8.0 Hz), 10.09 (s, 1H). HRMS. Calcd for  $\text{C}_{10}\text{H}_8\text{NO}_3$ ,  $[\text{M}+\text{H}]^+$ :  $m/z$  190.0504. Found:  $m/z$  190.0509.

### 4-(6-Bromo-7-hydroxybenzothiazol-2-yl)-6,8-dichloro-2H-chromen-2-one (5a)

A mixture of compound **4a** (1.33 g, 5.5 mmol) and compound **2** (1.1 g, 5 mmol) was heated under reflux in glacial acetic acid (10 mL) for 6 h, then cooled and diluted with water (50 mL). The resultant precipitate was purified by column chromatography using 1% methanol in dichloromethane as eluent to give **5a** as a yellow solid; yield 69%; mp 188–190°C;  $^1\text{H}$  NMR:  $\delta$  5.07 (s, 1H), 6.46 (s, 1H), 6.99 (s, 1H), 7.08 (s, 1H), 7.51 (d, 1H,  $J$ =8.2 Hz), 7.83 (d, 1H,  $J$ =8.2 Hz);  $^{13}\text{C}$  NMR:  $\delta$  118.7, 122.3, 124.8, 125.9, 126.9, 127.7, 129.8, 130.0, 132.4, 132.8, 133.1, 140.5, 145.1, 146.3, 155.1, 163.9. HRMS. Calcd for  $\text{C}_{16}\text{H}_7\text{BrCl}_2\text{NO}_3\text{S}$ ,  $[\text{M}+\text{H}]^+$ :  $m/z$  441.8707. Found:  $m/z$  441.8709.

### 4-(6-Bromo-7-hydroxybenzothiazol-2-yl)-6,8-dimethoxy-7-methyl-2H-chromen-2-one (5b)

Using the procedure for the preparation of **5a**, the reaction of **4b** (1.36 g, 5.5 mmol) and compound **2** (1.1 g, 5 mmol) gave **5b** as a yellow solid after purification by flash column chromatography using 2% methanol in dichloromethane as eluent; yield 66%, mp 188–190°C.  $^1\text{H}$  NMR:  $\delta$  2.27 (s, 3H), 3.71 (s, 3H), 3.76 (s, 3H), 5.45 (s, 1H), 6.83 (s, 1H), 7.01 (s, 1H), 7.42 (d, 1H,  $J$ =7.5 Hz), 7.69 (d, 1H,  $J$ =7.5 Hz);  $^{13}\text{C}$  NMR:  $\delta$  15.3, 57.4, 58.1, 119.4, 123.1, 125.2, 125.7, 125.9, 127.0, 128.9, 130.2, 131.5, 132.7, 135.8, 137.1, 143.1, 144.5, 157.9, 161.3. HRMS. Calcd for  $\text{C}_{19}\text{H}_{15}\text{BrNO}_5\text{S}$ ,  $[\text{M}+\text{H}]^+$ ,  $m/z$  447.9854. Found:  $m/z$  447.9853.

### 7-Amino-4-(6-bromo-7-hydroxybenzothiazol-2-yl)-2H-chromen-2-one (5c)

Using the procedure given for the preparation of **5a**, the reaction of **4c** (1.04 g, 5.5 mmol) and compound **2** (1.1 g, 5 mmol) gave **5c** as a deep yellow solid after purification by flash column chromatography using 5% methanol in dichloromethane as eluent; yield 79%, mp 170–172°C;  $^1\text{H}$  NMR:  $\delta$  5.53 (s, 1H), 6.21 (s, 1H), 6.51 (s, 2H), 6.92 (s, 1H), 7.01–7.09 (m, 2H), 7.55 (d, 1H,  $J$ =7.9 Hz), 7.85 (d, 1H,  $J$ =7.9 Hz);  $^{13}\text{C}$  NMR:  $\delta$  120.5, 122.3, 125.6, 125.8, 126.4, 127.0, 132.1, 132.3, 134.2, 134.7, 135.3, 139.6, 142.4, 144.6, 156.2, 162.9. HRMS. Calcd for  $\text{C}_{16}\text{H}_{10}\text{BrN}_2\text{O}_3\text{S}$ ,  $[\text{M}+\text{H}]^+$ :  $m/z$  388.9595. Found:  $m/z$  388.9590.

**Acknowledgment:** The author thanks the National Cancer Institute, Bethesda, MD, USA for performing the antitumor screening.

## References

- [1] Bojarova, P.; Kren, V. Glycosidases: a key to tailored carbohydrates. *Trends Biotechnol.* **2009**, *27*, 199–209.
- [2] Bruni, C. B.; Sica, V.; Auricchio, F.; Covelli, I. Further kinetic and structural characterization of the lysosomal  $\alpha$ -D-glucosidase glucohydrolase from cattle liver. *Biochim. Biophys. Acta* **1970**, *212*, 470–477.
- [3] Kalra, S. Alpha glucosidase inhibitors. *J. Pak. Med. Assoc.* **2014**, *64*, 474–476.
- [4] Wang, G.; Peng, Y.; Xie, Z.; Wang, J.; Chen, M. Synthesis,  $\alpha$ -glucosidase inhibition and molecular docking studies of novel thiazolidine-2,4-dione or rhodanine derivatives. *Med. Chem. Commun.* **2017**, *8*, 1477–1484.
- [5] Jemal, A.; Siegel, R.; Ward, E.; Murray, T.; Xu, J.; Thun, M. Cancer statistics, 2007. *CA Cancer J. Clin.* **2007**, *57*, 43–66.
- [6] Abbot, V.; Sharma, P.; Dhiman, S.; Noolvi, M. N.; Patel, H.; Bhardwaj, V. Small hybrid heteroaromatics: resourceful biological tools in cancer research. *RSC Adv.* **2017**, *7*, 28313–28349.
- [7] Nepali, K.; Sharma, S.; Kumar, D.; Budhiraja, A.; Dhar, K. Anti-cancer hybrids-a patent survey. *Recent Pat. Anticancer Drug Discov.* **2014**, *9*, 303–339.
- [8] Singh, A.; Mhlongo, N.; Soliman, M. E. Anti-cancer glycosidase inhibitors from natural products: a computational and molecular modelling perspective. *Anticancer Agents Med. Chem.* **2015**, *15*, 933–946.
- [9] Hayyan, M.; Hashim, M. A.; AlNashef, I. M. Superoxide ion: generation and chemical implications. *Chem. Rev.* **2016**, *116*, 3029–3085.
- [10] Birben, E.; Sahiner, U. M.; Sackesen, C.; Erzurum, S.; Kalayci, O. Oxidative stress and antioxidant defense. *World Allergy Organ. J.* **2012**, *5*, 9–19.
- [11] Reuter, S.; Gupta, S. C.; Chaturvedi, M. M.; Aggarwal, B. B. Oxidative stress, inflammation, and cancer: how are they linked? *Free Radic. Biol. Med.* **2010**, *49*, 1603–1616.
- [12] Bubols, G.; Vianna Dda, R.; Medina-Remon, A.; von Poser, G.; Lamuela-Raventos, R. M.; Eifler-Lima, V. L.; Garcia, S. C. The antioxidant activity of coumarins and flavonoids. *Mini Rev. Med. Chem.* **2013**, *13*, 318–334.
- [13] Kadhum, A. A.; Al-Amiry, A. A.; Musa, A. Y.; Mohamad, A. B. The antioxidant activity of new coumarin derivatives. *Int. J. Mol. Sci.* **2011**, *12*, 5747–5761.
- [14] Emami, S.; Dadashpour, S. Current developments of coumarin-based anti-cancer agents in medicinal chemistry. *Eur. J. Med. Chem.* **2015**, *102*, 611–630.
- [15] Proenca, C.; Freitas, M.; Ribeiro, D.; Oliveira, E. F.; Sousa, J. L.; Tome, S. M.; Ramos, M. J.; Silva, A. M.; Fernandes, P. A.; Fernandes, E.  $\alpha$ -Glucosidase inhibition by flavonoids: an in vitro and in silico structure-activity relationship study. *J. Enz. Inhib. Med. Chem.* **2017**, *32*, 1216–1228.
- [16] Taha, M.; Shah, S. A.; Afifi, M.; Imran, S.; Sultan, S.; Rahim, F.; Khan, K. M. Synthesis,  $\alpha$ -glucosidase inhibition and molecular docking study of coumarin-based derivatives. *Bioorg. Chem.* **2018**, *77*, 586–592.
- [17] Uremis, N.; Uremis, M. M.; Tolun, F. I.; Ceylan, M.; Doganer, A.; Kurt, A. H. Synthesis of 2-substituted benzothiazole derivatives and their in vitro anticancer effects and antioxidant activities against pancreatic cancer cells. *Anticancer Res.* **2017**, *37*, 6381–6389.
- [18] Gabr, M. T.; El-Gohary, N. S.; El-Bendary, E. R.; El-Kerdawy, M. M. Structure-based drug design and biological evaluation of 2-acetamidobenzothiazole derivative as EGFR kinase inhibitor. *J. Enzyme Inhib. Med. Chem.* **2015**, *30*, 160–165.
- [19] Gong, Z.; Peng, Y.; Qiu, J.; Cao, A.; Wang, G.; Peng, Z. Synthesis, in vitro  $\alpha$ -glucosidase inhibitory activity and molecular docking studies of novel benzothiazole-triazole derivatives. *Molecules* **2017**, *22*, 1555.
- [20] Taha, M.; Ismail, N.; Lalani, S.; Fatmi, M.; Wahab, A.; Siddiqui, S.; Khan, K.; Imran, S.; Choudhary, M. I. Synthesis of novel inhibitors of  $\alpha$ -glucosidase based on the benzothiazole skeleton containing benzohydrazide moiety and their molecular docking studies. *Eur. J. Med. Chem.* **2015**, *92*, 387–400.
- [21] Kurihara, H.; Mitani, T.; Kawabata, J.; Takahasi, K. Two new bromophenols from the red alga *Odonthalia corymbifera*. *J. Nat. Prod.* **1999**, *62*, 882–884.
- [22] Kim, K. Y.; Nguyen, T. H.; Kurihara, H.; Kim, S. M.  $\alpha$ -Glucosidase inhibitory activity of bromophenol purified from the red alga *Polyopales lancifolia*. *J. Food. Sci.* **2010**, *75*, H145–H150.
- [23] Xu, X.; Song, F.; Wang, S.; Li, S.; Xiao, F.; Zhao, J.; Yang, Y.; Shang, S.; Yang, L.; Shi, J. Dibenzyl bromophenols with diverse dimerization patterns from the brown alga *Leathesia nana*. *J. Nat. Prod.* **2004**, *67*, 1661–1666.
- [24] Liu, M.; Zhang, W.; Wei, J.; Lin, X. Synthesis and  $\alpha$ -glucosidase inhibitory mechanisms of bis(2,3-dibromo-4,5-dihydroxybenzyl) ether, a potential marine bromophenol  $\alpha$ -glucosidase inhibitor. *Mar. Drugs* **2011**, *9*, 1554–1565.
- [25] Shen, Q.; Shao, J.; Peng, Q.; Zhang, W.; Ma, L.; Chan, A. S.; Gu, L. Hydroxycoumarin derivatives: novel and potent  $\alpha$ -glucosidase inhibitors. *J. Med. Chem.* **2010**, *53*, 8252–8259.
- [26] Lodge, J.; Maier, T.; Leibl, W.; Hoffmann, V.; Strater, N. Crystal structure of *Thermotoga maritima*  $\alpha$ -glucosidase AgIa defines a new clan of NAD<sup>+</sup>-dependent glycosidase. *J. Biol. Chem.* **2003**, *278*, 19151–19158.
- [27] Boyd, M. R.; Paull, K. D. Some practical considerations and applications of the national cancer institute *in vitro* anticancer drug discovery screen. *Drug Rev. Res.* **1995**, *34*, 91–109.
- [28] Rahim, F.; Malik, F.; Ullah, H.; Wadood, A.; Khan, F.; Javid, M.; Taha, M.; Rehman, W.; Rehman, A.; Khan, K. M. Isatin-based Schiff bases as inhibitors of  $\alpha$ -glucosidase: synthesis, characterization, *in vitro* evaluation and molecular docking studies. *Bioorg. Chem.* **2015**, *60*, 42–48.
- [29] Brand-Williams, W.; Cuvelier, M.-E.; Berset, C. L. Use of a free radical method to evaluate antioxidant activity. *LWT Food Sci. Technol.* **1995**, *28*, 25–30.
- [30] Gabr, M. T.; El-Gohary, N. S.; El-Bendary, E. R.; El-Kerdawy, M. M. EGFR tyrosine-kinase targeted compounds: *in vitro* antitumor activity and molecular modeling studies of new benzothiazole and pyrimido[2,1-*b*]benzothiazole derivatives. *EXCLI J.* **2014**, *13*, 573–585.